Mineral Processing & Extractive Metall. Rev., 35: 126–135, 2014

ISSN: 0882-7508 print/1547-7401 online
DOI: 10.1080/08827508.2012.706762

VACUUM CARBOTHERMIC REDUCTION OF ALUMINA

Martin Halmann[1], Aldo Steinfeld[2,3], Michael Epstein[4], and Irina Vishnevetsky[1]

[1]*Department of Environmental Sciences and Energy Research, Weizmann Institute of Science, Rehovot, Israel*

[2]*Department of Mechanical and Process Engineering, ETH Zurich, Zurich, Switzerland*

[3]*Solar Technology Laboratory, Paul Scherrer Institute, Villigen, Switzerland*

[4]*Solar Research Facilities Unit, Weizmann Institute of Science, Rehovot, Israel*

The current industrial production of aluminum from alumina is based on the electrochemical Hall-Héroult process, which has the drawbacks of high-greenhouse gas emissions, reaching up to 0.70 kg $CO_{2\text{-equiv}}$/kg Al, and large energy consumption, about 0.055 GJ/kg Al. An alternative process is the carbothermic reduction of alumina. Thermodynamic equilibrium calculations and experiments by induction furnace heating indicated that this reaction could be achieved under atmospheric pressure only above 2200°C. Lower required reaction temperatures can be achieved by alumina reduction under vacuum. This was experimentally demonstrated under simulated concentrated solar illumination and by induction furnace heating. By decreasing the CO partial pressure from 3.5 mbar to 0.2 mbar, the temperature required for almost complete reactant consumption could be decreased from 1800°C to 1550°C. Deposits condensed on the relatively cold reactor walls contained up to 71 wt% of Al. Almost pure aluminum was observed as Al drops, while a gray powder contained 60–80% Al and a yellow-orange powder contained only Al_4C_3, Al-oxycarbides and Al_2O_3.

Keywords: alumina, aluminum, carbon, carbon monoxide, carbothermic reduction, vacuum

INTRODUCTION

Aluminum is the most abundant metallic element found in the Earth's crust, amounting to 8.3% by weight of the crust. Aluminum metal has been first isolated in 1825 by the Danish chemist Hans Christian Ørsted. This metal, particularly its alloys, has become of considerable importance due to its unique properties of lightweight, high-thermal and electric conductivity, and corrosion resistance (Balomenos, Panias, and Paspaliaris 2011). Because of the high calorific value of aluminum, 31 MJ/kg Al, a future important role could be that of an energy carrier and energy storage material. Thus, the well-known alkaline decomposition of aluminum or

Address correspondence to Martin Halmann, Department of Environmental Sciences & Energy Research, Weizmann Institute of Science, Rehovot 76100, Israel. E-mail: m.halmann@weizmann.ac.il

aluminum alloys, such as Al-Si to release hydrogen:

$$2Al + 6H_2O = 2Al(OH)_3 + 3H_2. \quad (1)$$

could be applied for hydrogen fuel cells in the transportation sector (Soler et al. 2009; Shkolnikov, Zhuk, and Vlaskin 2011). The production of primary (new) aluminum is the largest in volume in the nonferrous metal industry. In 2010 the world primary aluminum production reached 24 million metric tons, accounting for 1% of the world anthropogenic greenhouse gas emissions, while the production of iron and steel contributed 5.4%. Current aluminum production is based on two main stages, developed in the late 19th century:

(a) The Bayer process for producing Al_2O_3 from a mixture of minerals composing the deposits of bauxite. A simplified overall equation describing this process is

$$Al_2O_3n \cdot H_2O + 2NaOH = 2NaAlO_2 + (n+1)H_2O \quad (2)$$

in which in the above forward reaction, carried out in digesters, the alumina is solubilized to sodium aluminate at temperatures of 140–240°C, while most of the oxides of iron, silicon, and titanium remain insoluble, and are separated as "red mud." The solution of sodium aluminate is then cooled to 45–70°C, resulting in the reverse reaction of Equation (2), with precipitation of hydrated alumina, which then is calcined at 1150–1300°C to Al_2O_3 (Shkolnikov, Zhuk, and Vlaskin 2011). The Bayer process often requires a stage of mineral beneficiation, which involves the removal of fines. It coproduces a strongly alkaline waste (red mud), which is a serious environmental hazard (major accident in Hungary, October 4, 2010), and also requires large areas. The Bayer process uses about 25% of the total energy consumption of aluminum production.

(b) The Hall-Héroult electrolytic smelting process for converting Al_2O_3 to Al. This high-temperature electrochemical process in molten cryolite using sacrificial carbon anodes (releasing CO_2), prepared from calcined coke with pitch as binder, has the drawbacks of considerable environmental pollution due to perfluorocarbon (PFC) release, high-greenhouse gas emissions, reaching 0.70 kg $CO_{2\text{-equiv}}$/kg Al even in modern smelters, and large electrical energy consumption, about 15.4 MWh (or 55.4 GJ) per metric ton Al. If the CO_2 emission from coal-fired electric power generation is included, the Hall-Héroult process may cause the emission of up to 8 kg $CO_{2\text{-equiv}}$/kg kg Al, while the Bayer process uses up to 0.035 GJ/ton Al (Balomenos, Panias, and Paspaliaris 2011; International Aluminium Institute 2009). In the present study, thermochemical equilibrium calculations were made using the FACTSAGE and HSC computer codes (Factsage 2012; Roine 2006). Reaction enthalphies were derived using the data of the National Institute of Standards and Technology (NIST).

REACTIONS AT ATMOSPHERIC PRESSURE

Considerable efforts had been applied to produce aluminum from alumina by the alternative process of the carbothermic reduction of alumina, according to the overall Equations (3) and (4) (Cox and Pigeon 1963; Murray, Steinfeld, and Fletcher 1995; Steinfeld 1997; Murray 1999; Choate and Green 2003, Fruehan, Li, and Cargin 2004; Choate and Green 2006; Halmann, Frei, and Steinfeld 2007),

$$Al_2O_3 + 3C = 2Al + 3CO \quad (3)$$

$$Al_2O_3 + 3CH_4 = 2Al + 3CO + 6H_2 \quad (4)$$

Thermodynamic equilibrium calculations and experiments by induction furnace heating indicated that these reactions could be achieved under atmospheric pressure only above 2200°C (Halmann, Frei, and Steinfeld 2007). The reduction of alumina to Al under Ar and CH_4 at atmospheric pressure according to Equation (4) had been studied by radio frequency generated induction-coupled plasma, at above 10,000°C. The reduction products collected on a water-cooled surface contained Al and Al_4C_3 (Rains and Kadlec 1970). The drawback of the very high-reaction temperature is partly compensated by producing syngas as a valuable byproduct and by not requiring vacuum pumping (Halmann, Frei, and Steinfeld 2012a). Experiments using mixtures of Al_2O_3 and charcoal under Ar at atmospheric pressure in a quartz-tube reactor heated for 30 s pulses from an 18 kW induction furnace resulted in the condensation on the cold region of the reactor tube of elementary Al, as well as variable amounts of Al_2O_3, Al_4C_3, and the oxycarbides Al_2OC and Al_4O_4C. In the best result in one of the experiments, the Al content in the deposit was 29% (Halmann, Frei, and Steinfeld 2007; Halmann, Frei, and Steinfeld 2011). A moving-bed electric arc furnace for carbothermic reduction of Al_2O_3 with petroleum coke was patented, producing Al containing only 9–12% Al_4C_3 (Kirby 1982; Kirby and Saavedra 1988).

REACTIONS UNDER VACUUM

According to the Le Chatelier principle, the extent of a gas producing chemical reaction should be favored by a decrease in the total gas pressure. Thus, under vacuum conditions, the equilibrium of Equation (3) should be shifted to the right and the onset temperature for the metal production should be significantly lowered. Thermodynamic equilibrium calculations indeed predict the advantage of much lower required reaction onset temperatures by alumina reduction under vacuum, as shown in Table 1 (Halmann, Frei, and Steinfeld 2011; Kruesi et al. 2011). This had been experimentally demonstrated under simulated concentrated solar illumination and by induction furnace heating (Vishnevetsky and Epstein 2011; Feng,

Table 1. Calculated onset temperatures for Al(g) production as function of vacuum pressure in the system $Al_2O_3 + 3C$

Pressure, bar	Temperature, K
1 bar	2258
0.5 bar	2190
0.1 bar	2037
0.01 bar	1855
1 mbar	1703
0.1 mbar	1575
0.01 mbar	1465
0.001 mbar	1370

Bin, and Dai 2011). The direct vacuum carbothermic reduction has also been applied to the alumina contained in bauxite (Goldin et al. 1998; Yang et al. 2010; Halmann, Epstein, and Steinfeld 2012b). In a study of the vacuum carbothermal processing of low-iron bauxite, a mixture of calcined bauxite and charcoal heated up to 1600°C at an initial pressure of 0.01 mbar in a corundum reactor tube resulted in the condensation of β-SiC, Al_4O_4C, Al, Al_4C_3, and α-alumina on the cold wall of the reactor, in a residue of α-alumina, TiC, and FeO in the hot zone of the reactor (Goldin et al. 1998). In a related study, the production of Al-Si alloys had been studied by the vacuum carbothermal reduction of bauxite tailings containing mainly Al_2O_3, SiO_2, and Fe_2O_3 in a graphite furnace at pressures down to 10^{-9} bar and temperatures up to 2000°C, resulting in the formation of an Al-Si-Fe alloy, as well as carbides, elementary Al, and Si. The proposed mechanism involves the intermediate formation and decomposition of carbides, in which the presence of Fe seemed to have a catalytic effect (Yang et al. 2010).

INDUCTION FURNACE EXPERIMENTS

Experiments with induction furnace heating, using a 25 kW desktop Induction Heater, at temperatures of 1400–1800°C, an argon carrier gas flow rate of 100 ml/min, a pumping speed of 250 m^3/h, and an average CO partial pressure from 0.03 mbar to 0.35 mbar were conducted. The experimental reactor was built at the Solar Research Unit, Weizmann Institute of Science. Details of an earlier experimental setup and of the reaction procedure had been reported (Vishnevetsky and Epstein 2011). In addition to the gas chromatograph, the setup has now been fitted with an IR gas analyzer (Ultramat 23, Siemens, Germany), as shown in Figure 1. Stoichiometric reaction mixtures were prepared from beech charcoal (Chemviron)

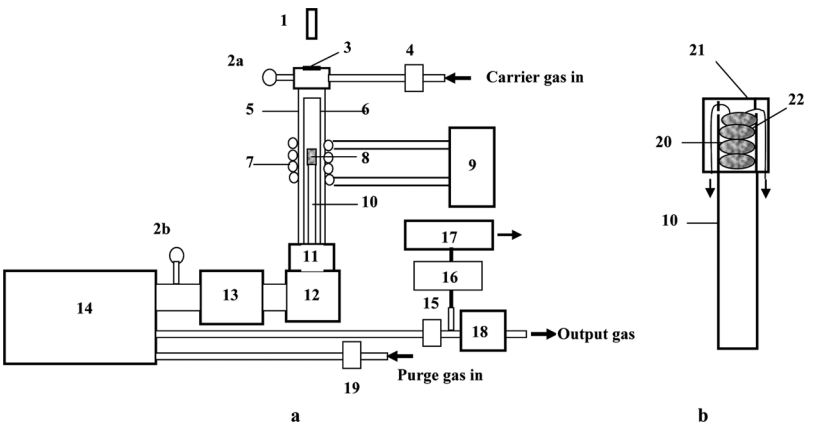

Figure 1. A scheme of the experimental setup: (a) 1-pyrometer, 2a.b-vacuum gauges, 3-quartz window, 4, 19-flow in controllers, 5-quartz tube, 6-zirconia tube, 7-induction coil, 8-graphite susceptor, 9-induction heater, 10-molybdenum tube with alumina insulation support, 11-water cooled trap, 12-filter, 13-liquid nitrogen trap, 14-dry vacuum system, 15-flow out meter, 16-diaphragm pump, 17-gas chromatograph, 18-IR analyzer; graphite susceptor and (b) 20-inner graphite crucible, 21-outer graphite crucible, and 22-reaction pellets.

Table 2. Amounts and composition of crucible residues after induction furnace heating

Test No.	Reaction temperature (°C)	Averaged CO partial pressure (mbar)	Initial Mass of reactant mixture (g)	Residue in crucible (g)	Content of residue
1	1406	0.03	3.83	1.52	80% Al_2O_3 17% Al_4C_3 3% Al_4O_4C
2	1453	0.1	3.30	0.15	74.5% Al_2O_3 25.5% Al_4CO_4
3	1602	0.18	2.70	<0.005	Graphite
4	1684	0.23	2.86	<0.005	65% Graphite 35% Al_4C_3
5	1606	1.45	3.53	0.85	27% Graphite 53% Al_4C_3 5% Al_4CO_4 15% Al_2O_3
6	1642	1.86	3.30	0.3	87% Al_4C_3 13% Graphite
7	1809	3.79	3.60	<0.005	Graphite

and 10-μm alumina powder (Sigma-Aldrich). Sugar (sucrose, 10 wt.%) was added as a binder. To prevent blowing losses, the mixture was pressed in reaction pellets. The pellets were then heated to 165°C, presumably resulting in caramelization of the sugar to sticky high-molecular weight compounds, which prevented the release of dust particles. Heating time up to the desired reaction temperature lasted 10–15 min and heating was stopped when the CO release reached zero. In tests at temperatures of about 1500–1600°C, with CO partial pressure 0.2–0.3 mbar, and at a temperature of 1800°C—with average CO partial pressure 3.5 mbar—the reactants were almost completely consumed in the forward reaction of alumina reduction, with only minor amounts of solids remaining in the reactor crucibles. At lower temperature or high-pressure residual amounts in the crucible were significantly larger and consisted of Al_4C_3, Al_4CO_4, graphite, and at the lowest test temperature, also, unreacted pellets covered by a carbide and oxycarbide layer (Table 2). Elementary aluminum could be observed as aluminum drops, or from 60–80% Al content in a gray powder (Figure 2). A yellow-orange powder contained

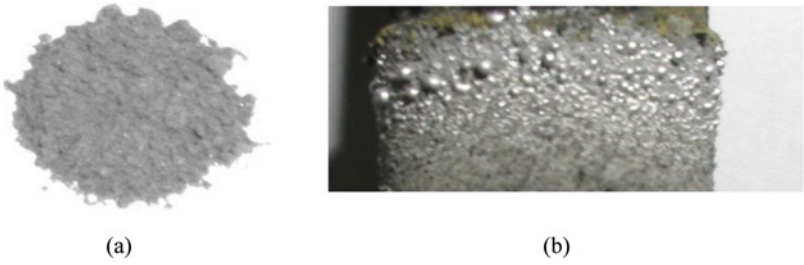

Figure 2. Example of deposits: (a) powder with 70% Al scraped from inner surface of zirconia tube and (b) aluminum drops condensed on molybdenum tube with OD = 20 mm (color figure available online).

Table 3. Results of quantitative analysis from profile-fitted peaks of XRD spectrum from a cold wall deposit

Product Species	Weight %
Aluminum, Al	70.9
Aluminum carbide, Al_4C_3	13.0
Aluminum oxycarbide, Al_4CO_4	10.7
Corundum, Al_2O_3	5.4

aluminum carbide, oxycarbide, and at lower reaction temperature also corundum, which could be formed together with aluminum from volatile aluminum suboxide Al_2O released as a byproduct if the temperature of the forward reaction was not high enough. The content of elementary Al in the deposits (59–71 wt.%) was measured by XRD quantitative analysis of profile-fitted peaks (see Table 3), using a Rigaku Ultima III diffractometer (Cu target), with data analysis performed by Jade 9.1 software. In the XRD spectrum shown in Figure 3, the products identified are indicated below the measured spectrum by the Powder Diffraction File (PDF) numbers and their major diffraction peaks, as listed by the ICDD (International Center for Diffraction Data). Aluminum vapors left the crucible and condensed on colder surfaces of the reactor, but which were still hot enough for the reverse reactions of carbonization and reoxidation of Al. The content of elementary aluminum at the deposition site depends on the rates of the reverse reactions and predominates in the outer layers of the deposit. The content of elementary aluminum at the deposition site depends on the rate of the reverse reaction.

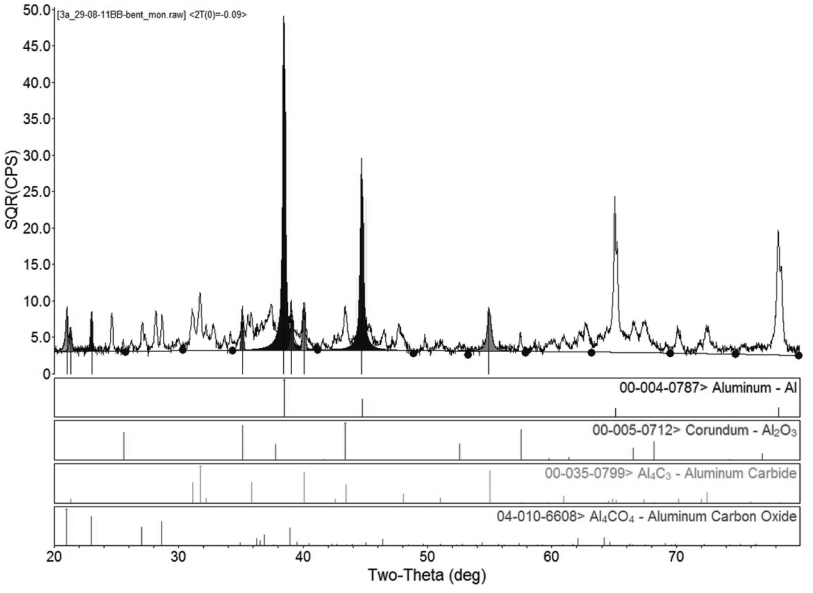

Figure 3. Upper section: XRD spectrum of deposit on the relatively cold surface of the reactor. Bottom section: Identified products with PDF numbers and their major diffraction peaks.

DISCUSSION

A major issue involved in aluminum carboreduction in vacuum is the actual electrical energy consumed by the vacuum pumps, which is substantially higher than the theoretical work of isothermal compression. The minimum theoretical work in isothermal expansion of the product gases, assumed to be brought from atmospheric pressure P_0 to vacuum pressure P is

$$\mathrm{W} = \mathrm{nRT_{reaction}lnP_0/P[kJ/molAl_2O_3]} \tag{5}$$

where n is the increase in the number of gas moles formed per mole of aluminum oxide including the amount of argon carrier gas moles, if any, $R = 8.\,314 \times 10^{-3}$ kJ $\mathrm{K^{-1}\,mol^{-1}}$ is the gas constant and $T_{reaction}$ is the absolute temperature of the reaction. The total net enthalpy input can be estimated from

$$\begin{aligned}\Delta\mathrm{H} = {} & \mathrm{H_{2al}(T_{reaction})} + \mathrm{H_{3CO}(T_{reaction})} + \mathrm{H_{kAr}(T_{reaction})} \\ & - \mathrm{H_{Al_2O_3}(20^{\circ}C)} - \mathrm{H_{3C}(20C)} - \mathrm{H^{kAr}(20^{\circ}C)}\end{aligned} \tag{6}$$

The hypothetical heat input for the reaction of Equation (3) to $2\mathrm{Al(g)} + 3\mathrm{CO(g)}$ at $\mathrm{T} = 1800^{\circ}\mathrm{K}$ without carrier gas was calculated to be 2,242 kJ/mol Al_2O_3. The minimum work of expansion from normal pressure to $P = 10^{-4}$ bar is 689 kJ/mol Al_2O_3. The total theoretical energy input would be 0.054 GJ/kg Al, comparable to that in modern smelters by the Hall-Héroult process of about 0.052 GJ/kg Al (Balomenos, Panias, and Paspaliaris 2011). At higher reaction temperature $2000^{\circ}\mathrm{K}$ and 1 mbar pressure, the total theoretical energy is 0.0522 GJ/kg Al, which also is similar to the energy consumption in the industrial process. However, the real pumping energy consumption can significantly exceed the theoretical work of exothermal expansion and at a CO partial pressure of less than 0.2–0.3 mbar (depending on amount of carrier gas used), the actual pumping energy would exceed the energy consumed in the industrial Hall-Héroult process, which in itself is at least two times higher than the theoretical figure, which is 0.023 GJ/kg Al (Beck 2011). The pumping energy was estimated (according to the Vacuum Technology Book 2011) for a dry vacuum system based on a Roots blower and a multi-stage Roots backing pump. As shown in Figure 4, to attain a pumping energy lower than the energy consumption in the current industrial process, the operating pressure must be higher than about 0.2 mbar. In order that the total energy input into the process (pumping plus the process heat and the sensible heat to bring the reactants to the reaction temperature) will be similar to the industrial process (curve 5 in Figure 4), the operating pressure must be higher than about 0.2 mbar (curves 3a,b,c. in Figure 4; curve 3b was taken as an example representing 1:1 molar ratio of argon as carrier gas to CO). In order that the total energy input into the process (pumping that consumes electricity plus the process heat and the sensible heat to bring the reactants to the reaction temperature, which is contributed by solar energy; see curves 4a,b,c in Figure 4) will be competitive to the current industrial process, the CO partial pressure should be higher than 1 mbar. According to the thermodynamic estimations, this entails an increase of about 200°C in the reaction temperature compared to operating at about 0.2 mbar. That was proved experimentally when the forward reaction was successfully completed during 20 min as the CO partial

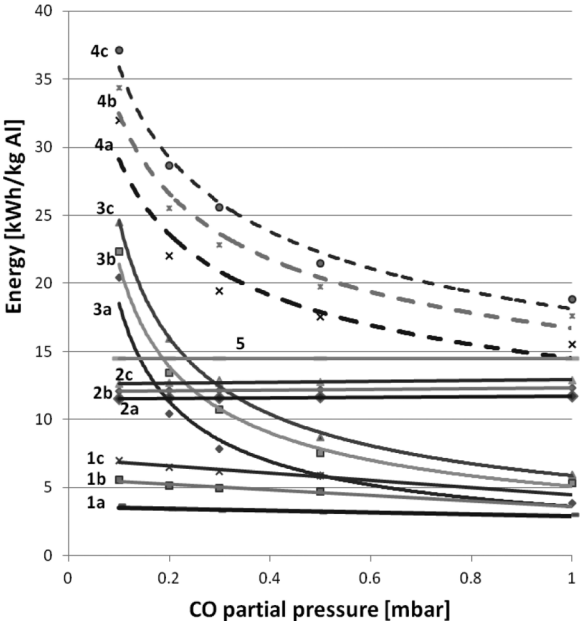

Figure 4. Real energy consumption for production of 1 kg Al/h as function of the CO partial pressure. 1-theoretical work for exothermal expansion; 2-net total process energy (chemistry plus sensible heat), 3-pumping energy; 4-total energy; 5-energy consumption in Hall-Héroult industrial electrolytic process (a-55.5 mol CO + 0 mol Ar/h, b-55.5 mol CO + 55.5 mol Ar, c-55.5 mol CO + 100 mol Ar).

pressure was increased from 0.18 mbar up to 3.79 mbar and the reaction temperature was increased from 1602°C to about 1809°C (see tests 3 and 7 in Table 2).

The main difficulty in the carbothermic reduction of alumina is of preventing the reoxidation or carbonization of the gaseous aluminum that condenses on the walls of the reactor where the temperature is still sufficiently high to promote the reverse reaction (e.g., the condensation temperature of aluminum vapors at 1 mbar pressure is 1546°C). XRD analyses of samples taken from different sites in the reactor confirm that the amount of elementary aluminum in the deposit strongly depends on the temperature at the specific site. The problem could be that at a continuous irradiation of the reaction crucible to a high temperature (1800°C), the forward reaction of Equation (3) is too fast relative to the rate of pumping out of the CO and of the Ar carrier gas. As a result aluminum vapor condenses on hotter areas and the residence time of the CO molecules is sufficient to allow them to react back. It is therefore important to design the pumping speed appropriately and in addition to the speed at the inlet of the pump, the resistance to flow in the connecting pipes, traps, etc, should be considered in order to obtain fast removal of the gases from the reactor. One possible approach would be to realize a reactor design, which maximally decreases the hot transition zone between the high-temperature reaction zone and the water-cooled area, where most of aluminum vapor should be condensed. Concentrated solar energy could be used to provide the energy required to preheat the reactor and the reactants to the operating temperature and to supply the endothermic energy required for the chemical reaction (Murray 1999; Kruesi et al. 2011).

ACKNOWLEDGMENT

The research leading to these results has received partial funding from the European Union Seventh Framework Programme (FP7/2007-2013) under grant agreement ENER/FP7EN/249710/ENEXAL. The authors thank the technical staff: Mr. Adi Arnon, Mr. Izhar Adikmann, and Mr. Shmuel Barak of the Weizmann Institute of Science Solar Research Unit for the construction of the experimental setup and assistance in preparing and carrying out the experiments, Dr. Yishay Feldman of the Weizmann Institute of Science Chemical Support Unit for the XRD measurements, and Mr. Rachamim Rubin for help with the calculations.

REFERENCES

Balomenos, E., Panias, D., and Paspaliaris, J., 2011, "Energy and energy analysis of the primary aluminium production processes – a review on current and future sustainability." *Mineral Processing and Extractive Metallurgy Review*, 32, pp. 69–89.

Beck, T. R., 2008, "Electrolytic production of aluminum." *Electrochemistry Encyclopedia*. Available at: http://electrochem.cwru.edu/encycl/art-a01-al-prod.htm

Choate, W. T. and Green, J. A. S., 2003. "U.S. energy requirements for aluminum production, historical perspective, theoretical limits and new opportunities." Available at: http://www1.eere.energy.gov/industry/aluminum/pdfs/al_theoretical.pdf

Choate, W. T. and Green, J., 2006, "Technoeconomic assessment of the carbothermic reduction process for aluminum production." *Light Metals*, pp. 445–450.

Cox, J. H. and Pidgeon, L. M., 1963, "The aluminum-oxygen-carbon system." *Canadian Journal of Chemistry*, 41, pp. 671–683.

FactSage Thermochemical Software & Database Package, October 2012, Centre for Research in Computational Thermochemistry, Ecole Polytechnique de Montreal, Canada. Available at: http://www.crct.polymtl.ca.

Feng, Yue-bin, Yang, Bin, and Dai, Yong-Nian, 2011, "Carbothermal reduction of alumina in a vacuum." *Advanced Materials Research*, pp. 156–157; Switzerland: Trans. Tech. Publications, pp. 1688–1691.

Fruehan, T. J., Li, Y., and Cargin, G., 2004, "Mechanism and rate of reaction of Al_2O, Al, and CO vapors with carbon." *Metallurgical and Materials Transactions B*, 35B, pp. 617–623.

Goldin, B. A., Grass, V. E., Ryabkov, and Yu, I., 1998, "Vacuum carbo-processing of low-iron bauxites." *Glass and Ceramics*, 55, pp. 323–325.

Halmann, M., Frei, A., and Steinfeld, A., 2007, "Carbothermal reduction of alumina: thermochemical equilibrium calculations and experimental investigation." *Energy*, 32, pp. 2420–2427.

Halmann, M., Frei, A., and Steinfeld, A., 2011, "Vacuum carbothermic reduction of Al_2O_3, BeO, MgO-CaO, TiO_2, ZrO_2, $HfO_2 + ZrO_2$, SiO_2, $SiO_2 + Fe_2O_3$, and GeO_2 to the metals. A thermodynamic study." *Mineral Processing and Extractive Metallurgy Review*, 32, pp. 247–266.

Halmann, M., Epstein, M., and Steinfeld, A., 2012a, "Carbothermic reduction of alumina by natural gas to aluminum and syngas: A thermodynamic study." *Minerals Processing and Extractive Metallurgy Review*, 33, pp. 352–361.

Halmann, M., Epstein, M., and Steinfeld, A. 2012b, "Bauxite components vacuum carbothermic reduction: a thermodynamic study." *Minerals Processing and Extractive Metallurgy Review*, 33, pp. 190–203.

International Aluminium Institute, 2009, "Aluminium for Future Generations/2009 Update." Available at: http://www.world-aluminium.org.

Kirby, R. M., 1982, "Carbothermic reduction furnace." US Patent 4,334,917.

Kirby, R. M. and Saavedra, A. F., 1988, "Viability of carbothermic alumina reduction." *Journal of Metals*, 40, pp. 32–36.

Kruesi, M., Galvez, M. E., Halmann, M., and Steinfeld, A., 2011, "Solar aluminum production by vacuum carbothermal reduction of alumina – thermodynamic and experimental analyses." *Metallurgical and Materials Transactions B, Process Metallurgy and Materials Processing Science*, 42, pp. 254–260.

Murray, J. P., 1999, "Aluminum production using high-temperature solar process heat." *Solar Energy*, 66, pp. 133–142.

Murray, J. P., Steinfeld, A., and Fletcher, E. A., 1995, "Metals, nitrides, and carbides via solar carbothermal reduction of metal oxides." *Energy*, 20, pp. 695–704.

National Institute of Standards and Technology, 2011, "NIST Standard Reference Database Number 69." *Standard Reference Data Program*, NIST Chemistry Webbook. Available at http://webbook.nist.gov/chemistry.

Rains, R. K. and Kadlec, R. H., 1970, "The reduction of Al_2O_3 to aluminum in a plasma." *Metallurgical and Materials Transactions B*, 1, pp. 1501–1506.

Roine A., October 2006, HSC Chemistry Computer Code V.6.0. Pori, Finland: Outokumpu Technology.

Soler, I., Candela, A. M., Macanas, J., Munoz, M., and Casado, J., 2009, "In situ generation of hydrogen from water by aluminium corrosion in solutions of sodium aluminate." *Journal of Power Sources*, 192, pp. 21–26.

Shkolnikov, E. I., Zhuk, A. Z., and Vlaskin, M. S., 2011, "Aluminum as energy carrier: Feasibility analysis and current technologies overview." *Renewable and Sustainable Energy Reviews*, 15, pp. 4611–4623.

Steinfeld, A., 1997, "High-temperature solar thermochemistry for CO_2 mitigation in the extractive metallurgical industry." *Energy*, 22, pp. 311–316.

Vacuum Technology Book, 2011, *Pfeiffer Vacuum (a catalogue)*, Vol. 1. Available at: www.pfeiffer-vacuum.net.

Vishnevetsky, I. and Epstein, M., 2011, "Metal oxides reduction in vacuum: setup development and first experimental results." Proceedings of SolarPaces Conference, Granada, Spain, September 20–23, pp. 20–23.

Yang, D., Feng, N.-X., Wang, Y.-W., and Wu, X.-I., 2010, "Preparation of primary Al-Si alloy from bauxite tailings by carbothermal reduction process." *Transactions of Nonferrous Metals Society of China* (in English), 20, pp. 147–152.